

## Neutrinos in gravitational collapse: Analysis of the flux profile

S V DHURANDHAR\* and C V VISHVESHWARA

Raman Research Institute, Bangalore 560080, India

\* Present Address: Tata Institute of Fundamental Research, Homi Bhabha Road,  
Bombay 400005, India

**Abstract.** The flux profile of the neutrinos emitted from a collapsing spherical object, as seen by a remote observer is studied. The model of the collapsing star consists of the Friedmann dust interior matched onto the Schwarzschild exterior. It is assumed that the neutrino emission occurs from an interior shell in a very short time interval. It is found that the nature of the flux profile falls into four distinct categories depending on the progress of collapse. Interesting features such as bursts, discontinuities, decay, etc are observed when the collapse has sufficiently progressed.

**Keywords.** Dense matter; neutrinos; collapsing stars; flux profile.

### 1. Introduction

In recent years, the influence of strong gravitational fields on neutrinos has been studied in different physical situations. A general relativistic description of neutrino transport in spherically symmetric, static compact objects was given by Kembhavi and Vishveshwara (1980). They examined the massless Dirac equation in the Schwarzschild interior matched onto the Schwarzschild exterior. Iyer *et al* (1982) investigated the behaviour of neutrinos in collapsing objects by employing the Dirac equation. This work complemented an earlier paper by Dhurandhar and Vishveshwara (1981) and yielded results strikingly similar to those of the latter although the formalisms followed in the two papers were different. The present study is a continuation of the work presented in the paper by Dhurandhar and Vishveshwara (1981) which will henceforth be referred to as paper I.

We shall assume the same idealized model of gravitational collapse and the corresponding background spacetime geometry as was considered in paper I. A spherically symmetric star undergoes collapse due to its own gravitational field and emits neutrinos from its interior. The interior geometry of the star is taken to be that of Friedmann dust (pressure zero) which is matched on to the Schwarzschild exterior metric at the surface of the star. In the range of energies considered, the neutrinos can be represented in the geometric optics limit to a good approximation, that is, the neutrinos can be assumed to describe null geodesics in the background geometry. The neutrino trajectories have been investigated in detail in paper I. The confinement (the capture of the neutrinos by the eventually formed blackhole) and the escape to infinity of the neutrinos have been examined in relation to the initial conditions during their emission.

In the present paper we apply these considerations to compute the flux of neutrinos as received by an observer sufficiently far away from the collapsing star. In §2 we derive an expression for  $I(t)$ , the neutrino flux as a function of the arrival time  $t$ . In §3 we first discuss the arrival time  $t$  as a function of the emission angle  $\psi$ . The nature of the

function  $t(\psi)$  depends crucially on the epoch at which the emission occurs. We then proceed to examine the flux profile  $I(t)$  based on the classification of  $\psi - t$  correlation. In the concluding section the significance of these results is discussed.

In as much as we have invoked the geometrical optics limit and assumed that null geodesics describe the paths of propagation, our formalism is applicable to any zero rest-mass particle or field and it is not necessarily confined to neutrinos. In this sense 'neutrino' can be treated as a generic term. The changing characteristics of the null geodesics and the energy flux carried by them not only act as probes of the evolving spacetime geometry, but also provide information on the collapse dynamics. However, throughout our discussions we have implicitly assumed that the infalling matter is transparent to the null geodesics in order to isolate only the general relativistic gravitational interaction. This assumption is not valid for photons. In the case of neutrinos there can exist astrophysical conditions under which our calculations are useful, perhaps with some modifications. All our computations would be relevant to the propagation of gravitational radiation generated by residual asymmetries inherent to the collapsing star. Thus, while we can hope that our results would be applicable to some realistic astrophysical situations, the problem we have studied is of significance in presenting a fully general relativistic picture of collapse dynamics as conveyed to a distant observer.

## 2. Derivation of the flux $I$ as a function of the arrival time $t$

### 2.1 Trajectory analysis

Before discussing the derivation proper, it is necessary to mention briefly the relevant quantities required.

The interior geometry (Friedmann dust) of the collapsing star is described by the line element,

$$ds^2 = dT^2 - S^2(T) [(1 - \alpha R^2)^{-1} dR^2 + R^2 (d\theta^2 + \sin^2 \theta d\phi^2)], \quad (1)$$

where  $c = 1$ ,  $G = 1$  and  $\alpha = 2m/R_b^3$ . Here  $(R, \theta, \phi)$  are the spatial coordinates which remain constant along the world line of the comoving observer and  $T$  the proper time. The  $R$ -coordinate of the particle on the boundary is  $R_b$ . The expansion factor  $S(T)$  is given by the parametric representation

$$\begin{aligned} S &= \cos^2 \chi, \\ T &= (\chi + \sin \chi \cos \chi) / \sqrt{\alpha}. \end{aligned} \quad (2)$$

The external geometry is Schwarzschild and is given by

$$ds^2 = \left(1 - \frac{2m}{r}\right) dt^2 - \left(1 - \frac{2m}{r}\right)^{-1} dr^2 - r^2 (d\theta^2 + \sin^2 \theta d\phi^2), \quad (3)$$

where  $m$  is the mass of the object in geometrical units. We match the components of the metric tensor of the two geometries and its derivatives at the boundary  $R = R_b$ . We have  $r = RS(T)$  and set  $t = 0$  when  $T = 0$ , that is the collapse begins at the Schwarzschild time  $t = 0$ . Owing to the spherical symmetry of the situation one can without loss of generality assume the trajectories to lie in the  $\theta = \pi/2$  plane. The null geodesics then depend essentially on three parameters namely  $R_0$  the radial coordinate

from which the neutrino is emitted,  $\chi_0$  the epoch of emission and  $\psi_0$  the angle the neutrino trajectory makes with the *outward* radial direction as measured by the comoving observer.

A brief account of the trajectories will be given here, a more detailed discussion being presented in paper I. Due to the various symmetries the first integrals are easily obtained, namely,

$$\begin{aligned} S \frac{dT}{d\lambda} &= \Gamma, \\ R^2 S^2 \frac{d\varphi}{d\lambda} &= h. \end{aligned} \quad (4)$$

The radial first integral is found to be

$$S^2 (dR/dT)^2 = (1 - \alpha R^2)(1 - B^2/R^2), \quad (5)$$

where

$$B = h/\Gamma = R_0 \sin \psi_0$$

is the impact parameter in the interior geometry.

In terms of the time coordinate  $\chi$ , (5) is integrated to provide the epoch  $\chi_b$  when the neutrino arrives at the boundary  $R = R_b$ . The value of  $\chi_b$  is given by

$$\chi_b = \begin{cases} \chi_0 + \frac{1}{4}[\chi_1(R_0) - \chi_1(R_b)] & \text{for } \psi_0 \leq \pi/2 \\ \chi_0 - \frac{1}{4}[\chi_1(R_0) - \chi_1(R_b)] + \pi/4 & \text{for } \psi_0 \geq \pi/2 \end{cases} \quad (6)$$

where

$$\chi_1(R) = \sin^{-1} \left( \frac{1 + \alpha R_0^2 \sin^2 \psi_0 - 2\alpha R^2}{1 - \alpha R_0^2 \sin^2 \psi_0} \right).$$

The time evolution of the trajectory may be continued to the point  $r = r_0$  in the Schwarzschild geometry well outside the object. The arrival time  $t$  of the particle at  $r_0$  is given by

$$t = t_b + \int_{r_b}^{r_0} \left(1 - \frac{2m}{r}\right)^{-1} \left[1 - \frac{b^2}{r^2} \left(1 - \frac{2m}{r}\right)\right]^{-1/2} dr, \quad (7)$$

where

$$r_b = R_b \cos^2 \chi_b, \quad (8)$$

$$\begin{aligned} t_b = & \left(\frac{R_b}{2m} - 1\right)^{\frac{1}{2}} (R_b + 4m)\chi_b + R_b \left(\frac{R_b}{2m} - 1\right)^{\frac{1}{2}} \sin \chi_b \cos \chi_b \\ & + 2m \ln \frac{\left(\frac{R_b}{2m} - 1\right)^{\frac{1}{2}} + \tan \chi_b}{\left(\frac{R_b}{2m} - 1\right)^{\frac{1}{2}} - \tan \chi_b} \end{aligned} \quad (9)$$

and  $b$  is the impact parameter of the particle in the Schwarzschild geometry. The time constant  $t_b$  is obtained from the following considerations. The collapse begins at  $t = 0$  from rest  $[(dr/dt)|_{t=0} = 0]$  and the particle on the boundary  $r = R_b$  describes a geodesic. This particle can be assigned both the time coordinates  $\chi_b$  and  $t_b$ . Then the relation between  $\chi_b$  and  $t_b$  can be obtained simply from the geodesic equations.

A similar analysis for the  $\varphi$ -coordinate of the particle trajectory yields the following

relations:

$$\varphi_b = \begin{cases} \varphi_0 - \frac{1}{2}[\varphi_1(R_b) - \varphi_1(R_0)] & \text{for } \psi_0 \leq \pi/2 \\ \varphi_0 + \frac{1}{2}[\varphi_1(R_b) + \varphi_1(R_0)] & \text{for } \psi_0 \geq \pi/2, \end{cases} \quad (10)$$

where

$$\varphi_1(R) = \sin^{-1} \left( \frac{1 + \alpha R_0^2 \sin^2 \psi_0 - 2(R_0^2/R^2) \sin^2 \psi_0}{1 - \alpha R_0^2 \sin^2 \psi_0} \right) \quad (11)$$

and

$$\varphi = \varphi_b \pm \int_{r_b}^{r_0} b r^{-2} \left[ 1 - \frac{b^2}{r^2} \left( 1 - \frac{2m}{r} \right) \right]^{-1/2} dr. \quad (12)$$

The matching of the metric components across the boundary of the object yields the Jacobian matrix between the interior and the exterior coordinate systems. Therefore the tangent vector components of the trajectory in the exterior geometry are determined in terms of the tangent vector components in the interior geometry. The relation between the time-components furnishes the spectral shift for the particle

$$1 + z = \frac{\cos^2 \chi_0}{\cos^2 \chi_b} \left[ (1 - \alpha R_b^2)^{\frac{1}{2}} - (\alpha)^{\frac{1}{2}} \tan \chi_b (R_b^2 - R_0^2 \sin^2 \psi_0)^{\frac{1}{2}} \right] \left( 1 - \frac{2m}{r_0} \right)^{\frac{1}{2}}. \quad (13)$$

The  $\varphi$ -components of the tangent vector at the boundary yield a relation between the two impact parameters  $B$  and  $b$ , namely,

$$b = B \cos^2 \chi_b / \left[ (1 - \alpha R_b^2)^{\frac{1}{2}} - (\alpha)^{\frac{1}{2}} \tan \chi_b (R_b^2 - R_0^2 \sin^2 \psi_0)^{\frac{1}{2}} \right]. \quad (14)$$

The radial velocity component at the boundary in the Schwarzschild geometry shows interesting behaviour. For  $\psi_0 \sim \pi/2$ ,  $R_0 \sim R_b$  and advanced epoch  $\chi_0$  the radial component of the velocity can assume negative values. This is the phenomenon of backward emission which has been fully analysed in paper I. The backward emission of the particle is responsible for a further delay in the arrival time.

## 2.2 The time variation of the flux

We assume that the emission of neutrinos takes place uniformly on a spherical shell lying inside the collapsing object; that is, the sources are of equal strength and that they are distributed uniformly over the entire shell. Further, it is assumed that the emission occurs in a 'flash', emitting a finite amount of energy in a very short time interval. Also each source sends out neutrinos isotropically as seen by the comoving observer in the Robertson-Walker geometry. Under these circumstances we investigate the flux of neutrinos as a function of time as seen by an observer sufficiently removed from the object.

In general,  $t$ , the arrival time of a neutrino at  $r = r_0$ , is a function of the initial parameters  $\chi_0$ ,  $R_0$  and  $\psi_0$ . But as we have assumed that the emission occurs at a single instant  $\chi_0$  and from a shell of fixed radius  $R_0$ , the arrival time  $t$  depends only on  $\psi_0$ . (Henceforth we drop the subscript 'zero' attached to the initial parameters). Therefore the variation of  $t$  with respect to  $\psi$  is of prime importance in our considerations. We shall discuss  $t$  as a function of  $\psi$  in the next section along with the flux profile. These two functions are closely related. This will be clear when we derive the expression for the flux as a function of the time of arrival.

In the general case the emission takes place from a shell of radius  $R \leq R_b$ . In order to simplify the geometry of the neutrino trajectories involved, which enter into our

derivation, we shall treat the case  $R = R_b$  in detail. For  $R < R_b$ , the geometry will be somewhat more complicated, but the derivation will follow the same pattern. Figure 1 shows the neutrino trajectories in the  $\theta = \pi/2$  hyperplane, projected on to the  $(r, \varphi)$  plane from the  $(t, r, \varphi)$  space. We consider a small element of area  $AB$  of the surface of the sphere  $r = r_0$  at the observer's position. We take the  $\varphi$ -coordinate of  $A$  to be zero. Let  $\delta\varphi$  be the height of the elementary area  $AB$ . We now consider all those neutrinos which pass through this area between the time instants  $t$  and  $t + \Delta t$ . The energy  $\Delta E$  of these neutrinos is computed and the flux  $I(t)$  follows on taking the limit of  $\Delta E/\Delta t$  as  $\Delta t$  tends to zero.

We assume for the time being that  $t$  is a strictly monotonically increasing function of  $\psi$ . In general this is not the case but the expression for  $I(t)$  then, can be obtained in an obvious manner from the simpler case which we treat now.

We choose points  $A'$  and  $B'$  on the shell  $R = R_b$  in the following manner. The null geodesic emanating from  $A'$  passes through  $A$  at time  $t$  and the null geodesic from  $B'$  reaches  $B$  at  $t + \Delta t$ . Let  $OA'$  make an angle  $\varphi$  with  $OA$ . Let  $\Delta\psi$  be the angle corresponding to  $\Delta t$ , that is, the neutrinos emitted between  $\psi$  and  $\psi + \Delta\psi$  reach the sphere  $r = r_0$  between  $t$  and  $t + \Delta t$ . Also as  $\varphi$  is a function of  $\psi$ , one can associate an angle  $\Delta\varphi$  with  $\Delta\psi$  and hence with  $\Delta t$ . Since there is spherical symmetry, the null geodesics can be rotated about the origin  $O$ . Then it is easy to check that the angle between  $OA'$  and  $OB'$  is  $\Delta\varphi + \delta\varphi$ .  $B'$  has the  $\varphi$ -coordinate  $\varphi + \Delta\varphi + \delta\varphi$ . Only those neutrinos emitted between the points  $A'$  and  $B'$  pass through  $AB$  during the specified time interval  $[t, t + \Delta t]$ . One can see, however, that for emission sources lying at an angular distance less than  $\delta\varphi$  from either  $A'$  or  $B'$ , the neutrinos pass through only a portion of the area  $AB$  in the specified time interval. But if we choose  $\delta\varphi \ll \Delta\varphi$  this contribution is negligible and may be omitted from our calculations. Let  $\delta\psi$  be the angle corresponding to  $\delta\varphi$  for an emission source  $C'$  lying between  $A'$  and  $B'$ . The neutrinos emitted between  $\psi$  and  $\psi + \delta\psi$  will pass through  $AB$  somewhere within a very small time interval contained within  $t$  and  $t + \Delta t$ . If one rotates the diagram about  $OC'$

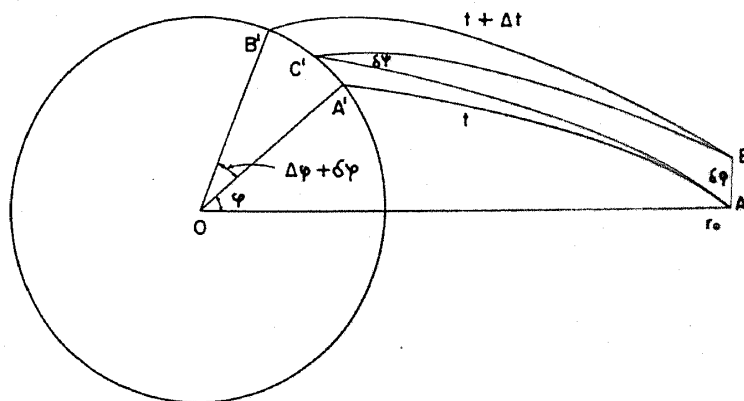


Figure 1. The figure shows the null geodesics emanating from  $A'$  and  $B'$  which reach  $A$  and  $B$  at times  $t$  and  $t + \Delta t$  respectively. The points  $A'$  and  $B'$  lie on the shell  $R = R_b$ , which has neutrino sources distributed uniformly over it.  $AB$  is the elemental area at  $r = r_0$  at the point of observation.  $C'$  is a typical point lying between  $A'$  and  $B'$  which emits neutrinos that pass through  $AB$  in a very small time interval lying between  $t$  and  $t + \Delta t$ . The angles  $\Delta\varphi + \delta\varphi$  subtended by the arc  $A'B'$  at  $O$  and  $\delta\psi$  between  $C'B$  and  $C'A$  have been exaggerated for the sake of clarity in the diagram.

one sees that an energy proportional to  $2\pi \sin \psi \delta\psi$  is distributed over the solid angle  $2\pi \sin \varphi \delta\varphi$  swept by  $AB$ . A similar rotation about  $OA$  shows that the number of sources which contribute to the flux at  $AB$  is proportional to  $2\pi \sin \varphi \Delta\varphi$ . Taking the spectral shift of the neutrinos  $(1+z)$  also into account it is possible to write the following expression for  $I(t)$ .

$$I(t) \Delta t \propto \frac{2\pi \sin \psi \delta\psi}{2\pi \sin \varphi \delta\varphi} \cdot 2\pi \sin \varphi \Delta\varphi (1+z)^{-1}.$$

Taking limits as both  $\Delta t$  and  $\delta\varphi$  tend to zero and omitting the constant factors we have the following result

$$I(t) = \frac{\sin \psi}{(1+z) dt/d\psi}. \quad (15)$$

In this derivation we have assumed that the emission occurs from the surface  $R = R_b$ . However, (15) remains valid for values of  $R$  less than  $R_b$ , where  $t$  and  $z$  are calculated using this value of  $R$ .

Secondly, when  $t$  is not a monotonic increasing function of  $\psi$  (15) has to be suitably modified. Fortunately, the alteration is simple. In our problem a single value of  $t$  corresponds at most to two values of  $\psi$  say  $\psi_1$  and  $\psi_2$ . The total flux  $I$  is then just a sum of the flux strengths corresponding to  $\psi_1$  and  $\psi_2$ . In the physical picture there are two rings of sources on the shell with  $\varphi$ -coordinates  $\varphi(\psi_1)$  and  $\varphi(\psi_2)$  which contribute to the flux at the time  $t$ . Thus, (15) in this case is replaced by

$$I(t) = \left[ \frac{\sin \psi}{(1+z) |dt/d\psi|} \right]_{\psi=\psi_1} + \left[ \frac{\sin \psi}{(1+z) |dt/d\psi|} \right]_{\psi=\psi_2}. \quad (16)$$

The modulus  $dt/d\psi$  is taken to ensure that the contribution from each term on the right side of (16) is non-negative.

It may be observed from (15) and (16) for  $I(t)$  that the arrival time  $t$  as a function of  $\psi$  requires a closer scrutiny. We devote the following section to this aspect and study its effect on the flux profile.

### 3. Discussion of the results

In this section we discuss the arrival time  $t$  of the neutrino as a function of the angle of emission  $\psi$ . Further, we apply these results to investigate the flux  $I$  as a function of the arrival time  $t$ . The discussion may be divided into four cases. We take up each case in chronological order, beginning with the start of the collapse.

#### Case (a)

We examine the situation in the early stages of the collapse. In this case the gravitational effects are minimal. There is no confinement of the neutrinos or any delay in their time of arrival due to the neutrinos circling around the collapsing object. The scenario is not dissimilar from the one in the absence of gravitational field. Both  $t(\psi)$  and  $I(t)$  are monotonic increasing functions of their respective arguments. Both these functions are

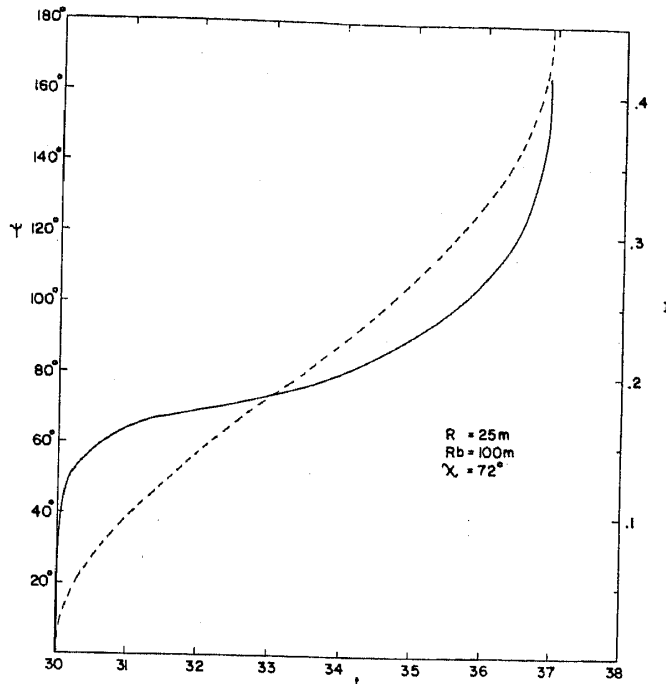


Figure 2 a. The undashed curve of the unscaled flux-intensity  $I$  is depicted in the figure as a function of the arrival time  $t$  for the early stages of the collapse. The flux intensity is seen to grow monotonically until finally it abruptly falls to zero. The dashed curve shows the  $\psi - t$  correlation.

depicted in figure 2a. The greater the value of  $\psi$  the longer it takes the neutrino to reach  $r_0$  with the neutrino having emission angle  $\psi = \pi$  arriving last at  $t = t_\pi$ .  $I(t)$  gradually increases with  $t$  until at  $t = t_\pi$  the flux abruptly falls to zero. One also observes that the slope of the curve  $t = t(\psi)$  becomes zero at  $\psi = \pi$ . Indeed, differentiating (7) with respect to  $\psi$ , we have,

$$\frac{dt}{d\psi} = \frac{dt_b}{d\chi_b} \frac{d\chi_b}{d\psi} + b \frac{db}{d\psi} \int_{r_b}^{r_0} \frac{dr}{r^2 \left\{ 1 - \frac{b^2}{r^2} \left( 1 - \frac{2m}{r} \right) \right\}^{\frac{3}{2}}} - \frac{dr_b}{d\psi} \left\{ \left( 1 - \frac{2m}{r_b} \right) \sqrt{1 - \frac{b^2}{r_b^2} \left( 1 - \frac{2m}{r_b} \right)} \right\}^{-1} \quad (17)$$

We note that  $(d\chi_b/d\psi)|_{\psi=\pi} = (dr_b/d\psi)|_{\psi=\pi} = 0$ .

Also  $b = 0$ , since the neutrino with  $\psi = \pi$  travels radially. This shows that  $(dt/d\psi)$  vanishes at  $\psi = \pi$ .

From (15) it might seem that the flux strength grows without bound as  $\psi$  approaches  $\pi$ . However, one must bear in mind that  $\sin \psi$  also vanishes as  $\psi$  tends to  $\pi$  and hence it is necessary to evaluate the limit  $\sin \psi (dt/d\psi)^{-1}$ . This limit which is essentially  $[(d^2t/d\psi^2)|_{\psi=\pi}]^{-1}$  turns out to be finite and negative in value during the early stages of the collapse. In fact this case deals with the regime for which  $(d^2t/d\psi^2)|_{\psi=\pi}$  is negative. However, for a more advanced epoch  $(d^2t/d\psi^2)|_{\psi=\pi}$  vanishes and changes sign. This is discussed in case (b).

## Case (b)

We investigate the situation for more advanced epochs, and more precisely, when  $(d^2t/d\psi^2)|_{\psi=\pi}$  changes sign and becomes positive and  $t(\psi)$  remains finite for  $0 \leq \psi \leq \pi$ . A typical curve  $t(\psi)$  is shown in figure 2(b). As  $\psi$  varies from 0 to  $\pi$ , the time of arrival  $t$  at first increases monotonically, reaches a maximum at  $t = t_m$  and then decreases, finally attaining the slope zero at  $\psi = \pi$ . This behaviour of  $t(\psi)$  reflects on the shape of the flux profile. The flux profile possesses two distinctive features:

- (i) A burst which occurs at the tail end of the flux function.
- (ii) A discontinuous increase in the flux at  $t = t_\pi$ , where  $t$  denotes the arrival time of the neutrino emitted with  $\psi = \pi$ . The reason for the burst is that  $dt/d\psi$  vanishes at the maximum of the curve  $t = t(\psi)$ , consequently  $I(t)$  tends to infinity as  $t$  approaches  $t_m$  as can be seen from (15) or (16). The necessary condition for the burst to occur is that  $(d^2t/d\psi^2)|_{\psi=\pi}$  be positive. It may be remarked that this burst is a reflection of the fact that we have chosen the emission to occur in a 'flash', that is the flux at the source of emission is infinite.

The discontinuity in the flux function occurs for the following reason: For a fixed value of  $t < t_\pi$  the neutrinos which arrive at  $r_0$  at  $t$  are emitted from a single ring on the shell of neutrino sources. There is only one value of  $\psi$  and hence of  $\varphi$  which corresponds to the time of arrival  $t$ . Hence  $I(t)$  is given by (15). However, when  $t > t_\pi$ , there are two values of  $\psi$  and hence of  $\varphi$  which correspond to a fixed value of  $t$ . The neutrinos received are emitted from two rings on the shell in question. In this case  $I(t)$  is given by (16). We observe that  $I(t)$  is discontinuous at  $t = t_\pi$ . The discontinuity  $\Delta I$  in  $I(t)$  at  $t = t_\pi$  is given by the following expression.

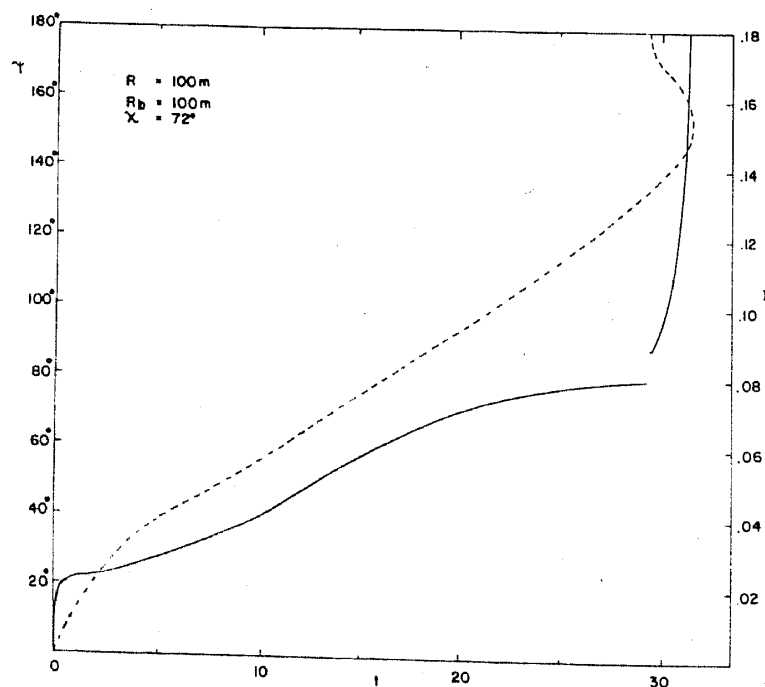


Figure 2 b. The figure shows that the dashed curve  $t(\psi)$  develops a maximum but remains finite. The undashed curve  $I(t)$  implies that the flux profile has a discontinuity and terminates in a burst.



$$\Delta I = \left\{ \left[ (1+z) \frac{d^2 t}{d\psi^2} \right]_{\psi=\pi} \right\}^{-1} \quad (18)$$

We now derive a relation between the epoch of emission and the shell radius when the function  $t(\psi)$  just begins to develop a maximum for  $\psi < \pi$ . It is of interest to examine the situation when the transition occurs from case (a) to case (b). The relation is obtained simply by setting,

$$(d^2 t/d\psi^2)|_{\psi=\pi} = 0. \quad (19)$$

Differentiating  $t$  with respect to  $\psi$  twice and then setting  $\psi = \pi$  one obtains the following result after a fair amount of calculation.

$$(d^2 t/d\psi^2)|_{\psi=\pi} = -\frac{2r_b(1-\alpha R_b^2)}{1-2m/r_b} - \frac{\sqrt{\alpha R}(R_b(1-\alpha R^2)^{\frac{1}{2}} + R(1-\alpha R_b^2)^{\frac{1}{2}}) \cos \chi_b \sin \chi_b}{1-2m/r_b} + \frac{R^2}{R_b^2} \left( \frac{r_b(1-r_0/r_b)}{((1-\alpha R_b^2)^{\frac{1}{2}} - \sqrt{\alpha R_b} \tan \chi_b)^2} \right), \quad (20)$$

where  $r_b$  and  $\chi_b$  are defined in (6) and (8) respectively. For a fixed value of  $R_b$  and  $r_0$ ,  $(d^2 t/d\psi^2)|_{\psi=\pi}$  is a function of  $R$  and  $\chi$ , that is the shell radius and the epoch of emission. Let  $F(R, \chi)$  denote this function, then (19) implies,

$$F(R, \chi) = 0. \quad (21)$$

For small values of  $R$  the first term in the right side of (20) dominates and the burst occurs at comparatively later stages.

In the extreme case of the emission occurring from the surface  $R = R_b$  the relation (21) reduces to,

$$1 - \frac{r_b}{r_0} - 2 \left(1 - \frac{2m}{R_b}\right)^{1/2} \left[ \left(1 - \frac{2m}{R_b}\right)^{1/2} - \left(\frac{2m}{R_b}\right)^{1/2} \tan \chi_b \right] = 0, \quad (22)$$

when  $r_b \ll r_0$ , one may neglect the second term in the left side of (22) to arrive at a simple result,

$$r_b = 8m \left(1 - \frac{2m}{R_b}\right). \quad (23)$$

This is the radius of the collapsing star when the neutrino emitted from the 'back' of the shell reaches the surface on the other side. If one further makes the approximation of  $R_b \gg m$ , it is possible to estimate the epoch when the emission occurred. One solves (23) for the emission epoch  $\chi$  in this approximation. The result in terms of the radius of the collapsing object at the epoch of emission turns out to be about 18  $m$ .

We have already remarked that the burst occurs because  $t(\psi)$  reaches a maximum. With the advance of epoch the maximum  $t = t_m$  of the curve  $t = t(\psi)$ , monotonically increases and the curve becomes more peaked. This process continues with the progress of collapse until as  $\chi$  approaches a certain value  $\chi_{dc}$ ,  $t_m$  tends to infinity (The subscript dc stands for double cone). In paper I we have seen that the confinement process occurs for neutrinos emitted between two distinct cones and they are prevented from escaping to

infinity. A thorough study of the conditions under which confinement occurs is made in paper I. The confinement process begins when the collapse has sufficiently advanced. The process starts with the direction of emission for which the particle is confined, lying in a coincident double cone. This cone gradually widens as the epoch is advanced with the inner cone becoming degenerate so that only a single cone remains. This single cone continues widening with the progress of the collapse. The confinement mechanism has been illustrated in figure 3 by exhibiting the cones at various stages of the collapse. This instant marking the beginning of the confinement process is represented by the epoch  $\chi_{dc}$ . Such neutrinos are forward emitted, having  $r_b < 3m$  and  $b \gtrsim 3\sqrt{3}m$ . As the epoch  $\chi$  approaches  $\chi_{dc}$ , the neutrinos emitted at the epoch  $\chi$  tend to increasingly circle the collapsing object in the vicinity of  $r \sim 3m$  and are therefore delayed in their transit. This behaviour causes the maximum of time of arrival  $t_m$  to increase without limit.

For the flux function  $I(t)$ ,  $t = t_m$  is an asymptote. Therefore when  $t_m$  tends to infinity as  $\chi$  approaches  $\chi_{dc}$ , the asymptote gets 'pushed' to infinity delaying the burst indefinitely.

The effect on the discontinuity at  $t = t_\pi$  is not as dramatic. As  $t_\pi$  increases steadily with the advance of epoch, the discontinuity occurs later and decreases in height.

Case (c)

In paper I it was shown that for  $\chi > \chi_{dc}$ , there exist values of the emission angle  $\psi$  for which the neutrinos are confined. For values of  $\chi \gtrsim \chi_{dc}$  and close to  $\chi_{dc}$ , those neutrinos are confined whose emission angles lie in the interval  $[\psi_1, \psi_2]$ . Neutrinos emitted in the directions enclosed by the cones with half angles  $\psi_1$  and  $\psi_2$  cannot escape to infinity; hence the nomenclature 'double cone confinement'. With the progress of collapse  $\psi_2$  finally attains the value  $\pi$  and at this epoch and later, only a single cone exists such that

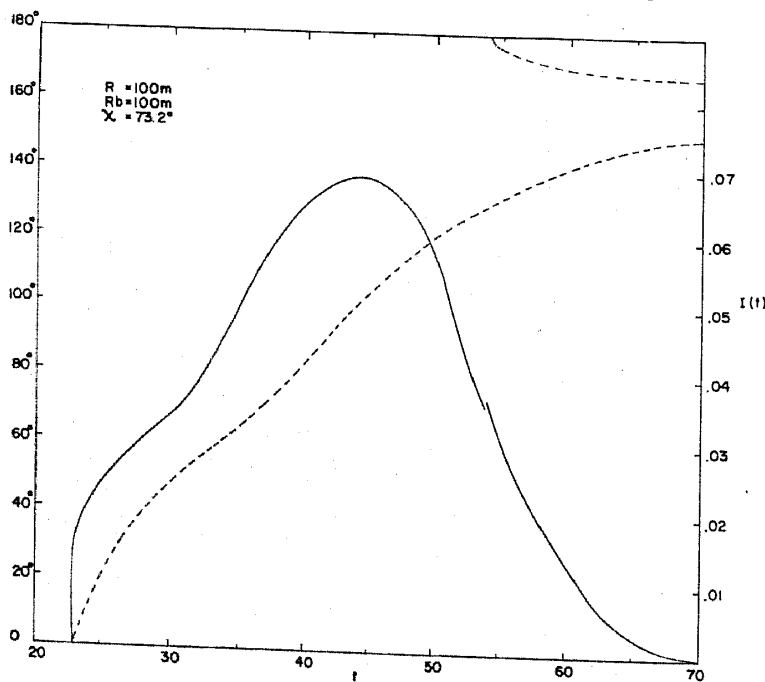


Figure 2c. The dashed curve  $t(\psi)$  tends to infinity as  $\psi$  approaches the critical values  $\psi_1$  and  $\psi_2$ . The undashed curve  $I(t)$  possesses a maximum and a discontinuity, which is smaller in height in comparison to case (b). The flux strength finally decays as  $t$  tends to infinity.

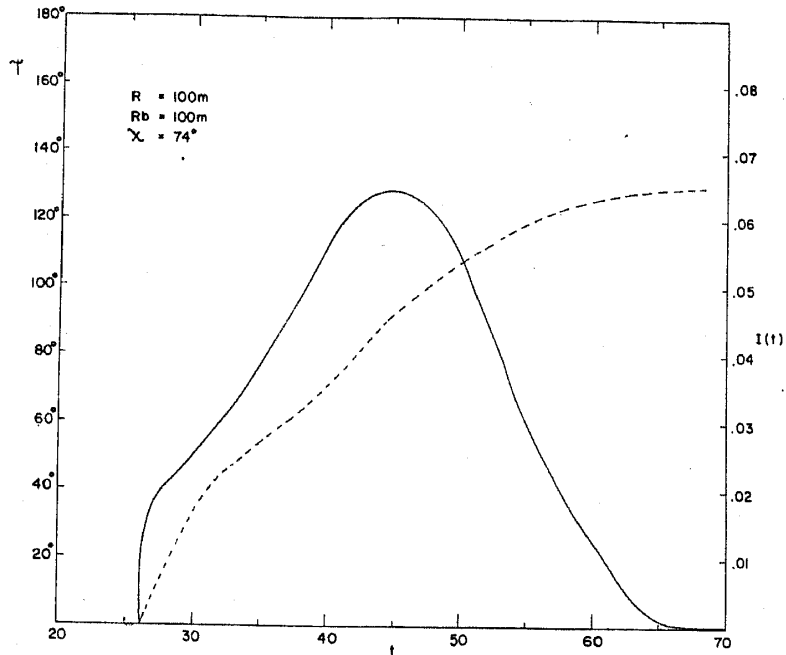


Figure 2 d. The dashed curve  $t(\psi)$  tends to infinity as  $\psi$  approaches a critical value  $\psi_1$ . The flux intensity  $I$  develops a maximum and then decays for large times  $t$ .

the neutrinos emitted within this cone will eventually fall into the blackhole. We call this epoch  $\chi_{sc}$  (the subscript sc denoting single cone). The case under discussion deals with the epochs  $\chi$  satisfying  $\chi_{dc} < \chi_0 < \chi_{sc}$ .

A typical curve  $t(\psi)$  for this case is shown in figure 3c. The curve possesses two asymptotes  $\psi = \psi_1$  and  $\psi = \psi_2$  which are the half-angles of the two cones. The time of arrival tends to infinity as  $\psi$  approaches either  $\psi_1$  or  $\psi_2$ .

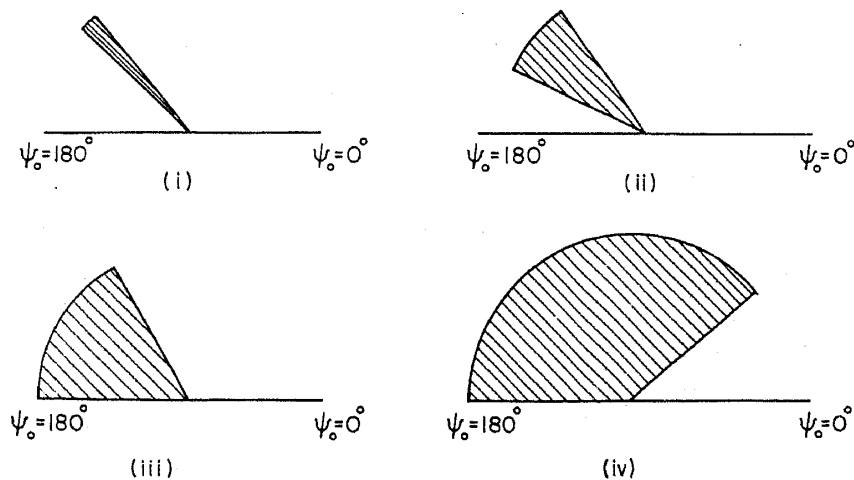


Figure 3. The shaded regions in the figure show the range of directions in the angle  $\psi_0$  for which confinement occurs. The four figures (i), (ii), (iii) and (iv) are drawn for progressive stages of the collapse. In figures (i) and (ii) the confinement directions are bounded by two cones while in (iii) and (iv) only one cone bounds the confinement directions.

One observes, that the function  $I(t)$  remains bounded, that is, the burst is absent. However, as the neutrinos with  $\psi_2 < \psi \leq \pi$  reach the observer at  $r_0$  the flux function still possesses the discontinuity at  $t = t_\pi$ . Since  $t_\pi$  is an increasing function of the epoch the discontinuous jump in the flux is delayed and also diminished in size as compared with case (b). In fact as the epoch  $\chi$  approaches  $\chi_{sc}$ ,  $r_b$  approaches  $2m$  and as one can see from (7), the integral diverges logarithmically and therefore  $t_\pi$  tends to infinity. Thus the discontinuity is delayed without limit. A typical flux profile  $I(t)$  is shown in figure 2c.

One may remark here that this phase of the collapse discussed under this case occurs for a very small fraction of the time taken for the entire collapse. For  $R_b \sim 100m$ ,  $\chi_{sc} - \chi_{dc} \sim 10^{-2}$  radians.

#### Case (d)

This part of the discussion deals with the last stages of the collapse when the epoch of emission  $\chi > \chi_{sc}$ . To get an idea of the numbers involved, if the initial radius  $R_b \sim 100m$  and if the emission occurs from the surface then  $R_b \cos^2 \chi_{sc}$ , the radius of the object during emission is about  $8m$ . In this case there is single cone confinement, that is, there exists a  $\psi_1$  such that for  $\psi > \psi_1$  the neutrinos are swallowed up by the incipient blackhole while for  $\psi < \psi_1$  the neutrinos escape to infinity.  $\psi_1$  is a decreasing function of the epoch  $\chi$ . For surface emission the maximum value of  $\psi_1$  is obtained when the epoch is  $\chi_{sc}$ . In particular, for  $R_b \sim 100m$ ,  $\psi_1 \sim 140^\circ$ .

The arrival time  $t$  is a monotonic increasing function of  $\psi$  in the permissible range  $0 \leq \psi < \psi_1$ . As  $\psi$  tends to  $\psi_1$ ,  $t$  tends to infinity  $\psi = \psi_1$  is an asymptote to the curve. This behaviour of  $t(\psi)$  gives rise to the following nature of the curve  $I(t)$ . Initially the flux  $I$  increases in value, reaches a maximum and then gradually decays for large values of  $t$ . Figure 2d depicts the function  $t(\psi)$  and the flux  $I(t)$ . Both the features of discontinuity in the flux profile and the tail end burst are absent in this case.

It is conjectured from numerical computations that these four categories in the behaviour of  $I(t)$  are present for all values of the radius  $R$  of the emitting shell. However, when the shell lies close to the surface these features seem to be more pronounced.

#### 4. Concluding remarks

In the foregoing we have analysed in detail the profile of the neutrino flux received by a distant observer. The form of the profile depends (changes) characteristically on the epoch at which the neutrinos are emitted during the collapse. We have studied the behaviour for different initial sizes of the collapsing object varying from a radius of  $100m$  to  $10m$ . The general features of the flux profile as a function of time remain basically unaltered. As we have seen, the nature of the flux falls into four distinct categories. For early stages of emission, when the gravitational effects are minimal, one observes a gradual rise and a sharp fall in the flux. On the other hand, if the collapse has reached an advanced stage, the flux after a gradual rise, decays slowly. Between these two extreme cases there are two separate intermediate stages both exhibiting discontinuities, with the earlier one ending in a burst. The progressive behaviour of the neutrino flux therefore indicates the size reached by the collapsing object at the moment

of emission. Thus the signature of the collapse process is impressed upon the escaping neutrinos.

**References**

- Dhurandhar S V and Vishveshwara C V 1981 *Astrophys. J.* **245** 1094  
Iyer B R, Dhurandhar S V and Vishveshwara C V 1982 *Phys. Rev.* **D25** 2053  
Kembhavi A K and Vishveshwara C V 1980 *Phys. Rev.* **D22** 2349